Precision spectroscopy and density-dependent frequency shifts in ultracold Sr

Tetsuya Ido, Thomas H. Loftus, Martin M. Boyd, Andrew D. Ludlow, Kevin W. Holman, and Jun Ye
JILA, National Institute of Standards and Technology and University of Colorado
Boulder, Colorado 80309-0440, U.S.A.

(Dated: February 2, 2008)

By varying the density of an ultracold ^{88}Sr sample from 10^9 cm^{-3} to $> 10^{12}$ cm^{-3}, we make the first definitive measurement of the density-related frequency shift and linewidth broadening of the $^1S_0$ - $^3P_1$ optical clock transition in an alkaline earth system. In addition, we report the most accurate measurement to date of the ^{88}Sr $^1S_0 - ^3P_1$ optical clock transition frequency. Including a detailed analysis of systematic errors, the frequency is $(434\ 829\ 121\ 312\ 334 \pm 20_{stat} \pm 33_{sys})$ Hz.

PACS numbers: 42.62.Eh; 32.80-t; 32.70.Jz; 42.62.Fi

arXiv:physics/0410110v2 [physics.atom-ph] 21 Jan 2005

Neutral-atom-based optical frequency standards are becoming serious contenders for the realization of highly stable and accurate optical atomic clocks [1, 2, 3]. Progress in this field is rapid, with significant advances in experimental techniques from several related fields including laser cooling to ultracold temperatures [4, 5, 6, 7], trapping configurations suitable for highly accurate clocks [3], the development of high quality optical local oscillators [8], and precise frequency measurement and distribution enabled by femtosecond optical combs [9, 10, 11].

Several systems have been proposed for neutral-atom-based optical clocks, each emphasizing narrow intercombination transitions in alkaline earth [1, 2, 12, 13, 14] and Yb atoms [15, 16]. High resolution spectroscopic techniques employed to date include recoil-free absorption inside 1-D optical lattices [13], free space Ramsey interrogation and atom interferometry [17], and free space saturated absorption [18]. The fermionic strontium isotope, ^{87}Sr, offers a weakly allowed $^1S_0$ - $^3P_0$ optical clock transition with a potential resonance quality factor exceeding 10^{15} and reduced polarization dependence and collisional shifts of the clock frequency when the atoms are confined inside magic-wavelength optical lattices [3, 19, 20]. However, the large nuclear spin ($I = 9/2$) brings complexity in state preparation and field control. Recently new schemes have emerged that take advantage of the most abundant spin-zero isotope (^{88}Sr) by engineering a $^1S_0$ - $^3P_0$ clock transition with a perfect scalar nature [21].

In this Letter, we present precision spectroscopy of ultracold ^{88}Sr in free space. With reference to the Cs primary standard and with a detailed investigation of systematic frequency shifts, we determine the absolute frequency of the $^1S_0 - ^3P_1$ clock transition with a statistical (systematic) uncertainty of 20(33) Hz. This level of measurement precision represents an improvement of more than 200 times over recent studies performed with thermal atomic beams [22]. Collision-related frequency shifts can significantly impact both the stability and accuracy of microwave and optical frequency standards. These effects have been studied in detail for both Cs and Rb microwave clocks [23, 24, 25]. For optical frequency standards based on intercombination transitions in alkaline earth atoms, it is expected that the dependence of the fractional frequency shift on the atomic density is reduced by more than three orders of magnitude in comparison to Cs clocks [26]. Previous efforts to measure this effect in Ca, however, were hampered by low sample densities $\sim 10^9$ cm^{-3}, resulting in measured shift coefficients with errors exceeding their associated absolute values [27]. To overcome this limitation, we have performed absolute frequency measurements with $\sim$1 μK ^{88}Sr atoms for densities spanning three orders of magnitude, from 10^9 cm^{-3} to 10^{12} cm^{-3}. For the first time we report definitive density-related line center shifts and spectral broadening of an optical clock transition in ultracold atoms. We find the density-dependent fractional frequency shift is 250 times smaller than that of Cs.

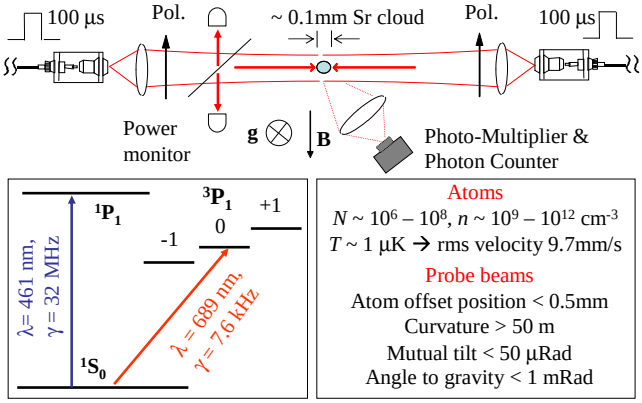

FIG. 1: (color online) Top view of the ultracold ^{88}Sr spectrometer. The two counter-propagating beams are collimated and overlapped. The beam intensities are balanced via atomic fluorescence signals. Light polarization is parallel to the bias magnetic field. A simplified ^{88}Sr level diagram and relevant experimental parameters are given in the bottom two panels.

Figure 1 shows a simplified view of the ultracold ^{88}Sr spectrometer. Components pertaining to atom cooling and trapping are described elsewhere [7, 28]. Measurements reported here utilize 10^6 to 10^8 atoms cooled to $\sim$ 1.3 μK. Spectroscopic probing of the $^1S_0$ - $^3P_1$ clock transition is performed in free space after the trapping

laser beams and the quadrupole magnetic field are ex tinguished. The atomic density n during spectroscopi probing is varied by changing either the initial atom num ber in the trap or the free-flight time after the atom are released to free space. The typical free-flight time range from 5 to 20 ms. Spatial densities are determine from calibrated fluorescence images. The probe lase linewidth is <100 Hz. The laser's absolute frequency i measured continuously via a femtosecond optical com that is locked to a Cs-referenced hydrogen maser via fiber optic link to NIST [31]. The probe laser is spli into two counter-propagating beams, each coupled re spectively into a single-mode, polarization-maintainin optical fiber before delivery to the atomic cloud. Th probe beams have $1/e$ diameters of 3 mm, > 50 m ra dius of curvature at the atom cloud, and are precisel overlapped (<50 μrad mutual tilt angle) by back cou pling each beam into the opposing beam's fiber launche Both beams are normal to gravity to within 1 mrad. T selectively probe the $^1S_0$ ($m_J = 0$) to $^3P_1$ ($m'_{J'} = 0$ transition, the linear probe beam polarization is paralle (within 10 mrad) to a $4.6(2)\times10^{-4}$ T bias magnetic fiel turned on during the measurement cycle. The counter propagating beam intensities are balanced to within 2.5% by monitoring atomic fluorescence signals. The singl beam intensity (steady-state saturation of ~ 1.1) corre sponds to a resonant π-pulse time of ~ 87 μs compare to the probe pulse duration of 100 μs. Each point in given trace of the atomic resonance is independently nor malized by the simultaneously measured atom number.

Before proceeding further it is important to emphasiz that the counter-propagating beam configuration is es sential to obtaining accurate values for the $^1S_0$ - $^3P_1$ lin center frequency. The ultracold ^{88}Sr temperature offers an advantage in reducing systematic frequency shifts as sociated with atomic motion. However, we find that due to trapping-beam-intensity imbalance the atomic cloud acquires typical drift velocities along the probe beam axis of $\sim$1 mm/s after release from the trap [29]. Although small, this drift corresponds to a frequency shift of 1.5 kHz if a single probe beam is used for the spectroscopy. This frequency offset is canceled without perturbing the line shape if the atomic sample is illuminated by two equal intensity, counter-propagating probe beams. The presence of both beams also enables cancellation of the first-order gravity-induced Doppler shift. For the more realistic $\pm$ 2.5% intensity balance achieved here, the line shape is unperturbed but the true line center remains uncertain by $\pm$ 20 Hz, an effect that could be eliminated in future measurements by using an optical cavity to es tablish the two probe beams. Although the two beam configuration described here resembles traditional satu rated absorption, the saturation effect is greatly reduced since the excitation pulse length is comparable to the spontaneous decay time (21 μs) while, for the ultra-cold temperatures employed here, the homogeneous and in homogeneous linewidths are comparable. We estimate the saturation effect causes a slight reduction of $\sim$ 1% of

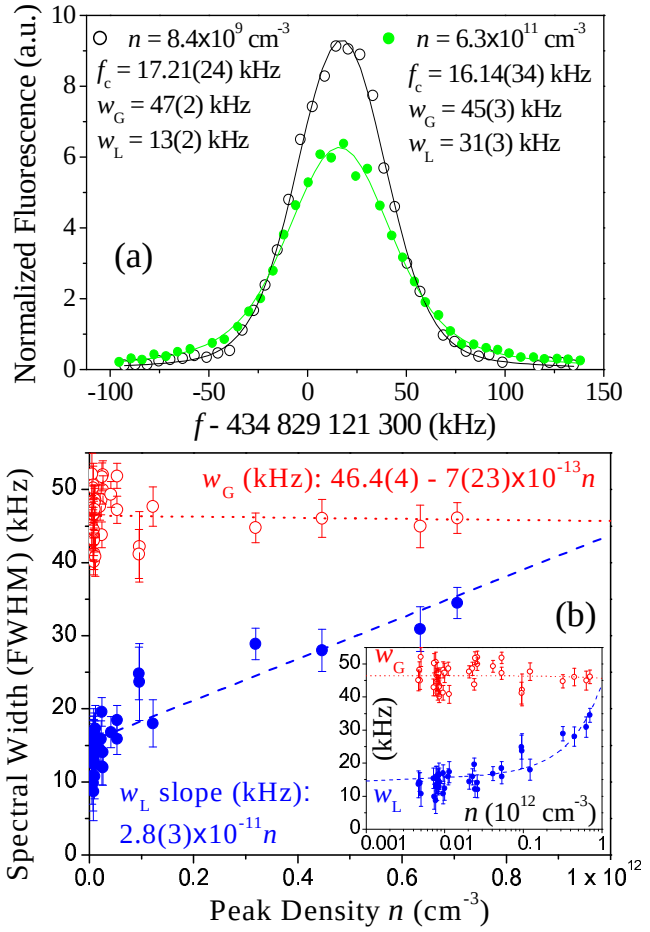

FIG. 2: (color online) Dependence of the $^1S_0 - ^3P_1$ transition linewidth on n for 10^9 cm^{-3} $< n <$ 10^{12} cm^{-3}. (a) Resonance profiles obtained for two different n. Circles represent data and the solid lines are fits to Voigt profiles. f_c, w_L, and w_G are the line center frequency, the Lorentzian linewidth, and the Gaussian linewidth, respectively. (b) w_L and w_G vs n, indicating a constant w_G and a linearly broadened w_L. The inset is a semi-log plot of the same data.

the fluorescence signal peak at ($\omega_0 + \omega_R$), where ω_R is the one photon-recoil frequency (2π 4775 Hz) and ω_0 the original atomic resonance. At the location of stimulated emission at (ω_0 - ω_R), the reduction of fluorescence signal is estimated to be $< 0.1\%$. Such a small deviation from the originally symmetrical lineshape causes a systematic shift in the measured resonance frequency by $\sim$ +4(20) Hz. Note also that Ramsey interrogation is not well suited to free-space measurements of the ^{88}Sr $^1S_0$ - $^3P_1$ transition as its linewidth is slightly larger than the single-photon recoil frequency. Hence the Ramsey time required to align the recoil components exceeds the excited state lifetime.

Figure 2 illustrates the dependence of the $^1S_0$ - $^3P_1$ transition linewidth on the peak density n for n ranging from 10^9 cm^{-3} to 10^{12} cm^{-3}. Figure 2(a) shows two typical resonance profiles obtained at densities of 8.4×10^9 cm^{-3} and 6.3×10^{11} cm^{-3}. The frequency axis is cali-

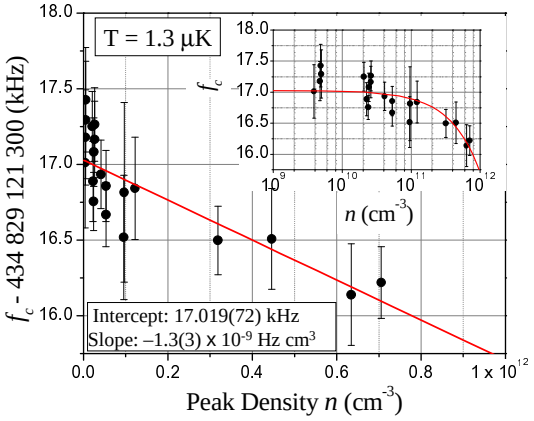

FIG. 3: Dependence of the $^1S_0 - ^3P_1$ transition line center on n. Filled circles (the solid line) are data (a linear fit). A fractional frequency shift of $-2.9(7) \times 10^{-24}$ cm^3 is determined. The inset is a semi-log plot of the same data.

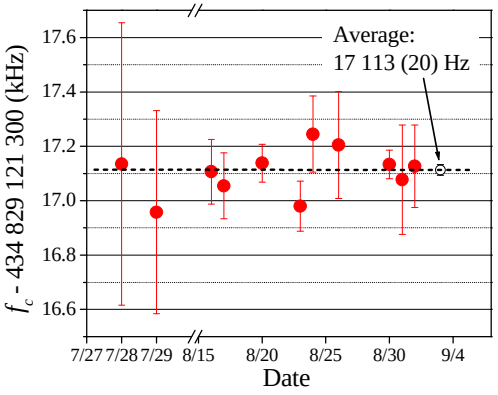

FIG. 4: Accumulated record of the zero density $^1S_0 - ^3P_1$ optical clock transition frequency. Each entry is a weighted mean of several independent measurements that are referenced to the NIST Cs fountain clock. The overall weighted mean value is (before correction for systematic shifts) 434 829 121 317 113 Hz, with a statistical uncertainty of 20 Hz.

brated with respect to the Cs standard. Circles represent experimental data while the solid lines are fits to Voigt profiles. The fits establish the line-center f_c, the Gaussian linewidth w_G, and the Lorentzian linewidth w_L. As n increases by a factor of ~ 80, both f_c and w_L change significantly beyond the associated measurement uncertainties. As expected, however, w_G remains essentially constant across the entire density range, as confirmed by the flat linear fit to the open circles in Fig. 2(b). The measured w_L, shown as filled circles in Fig. 2(b), demonstrates a significant linear broadening coefficient of $2.8(3) \times 10^{-8}$ Hz cm^3. The zero-density extrapolated linewidth of 14.5(5) kHz (Fig. 2(b) inset) agrees with the predicted linewidth of 13.6(5) kHz after considering power and interaction-time broadenings. In addition, we find that the integrated area under the Voigt profile, which is proportional to the number of photons per atom that contribute to the observed fluorescence signal, remains constant within the measurement uncertainty for $n < 5 \times 10^{11}$ cm^{-3}. For $n \geq 5 \times 10^{11}$ cm^{-3} (peak optical density of $\sim$ 4.5), however, the Voigt profile area decreases steadily with n, an effect that arises from probe beam attenuation and possibly radiation trapping.

Figure 3 summarizes the frequency shift of the $^1S_0$ - $^3P_1$ transition vs n for $n < 1 \times 10^{12}$ cm^{-3}. Filled circles (the solid line) are experimental data (a linear fit). From the fit we determine a fractional frequency shift of $-2.9(7) \times 10^{-24}$ cm^3, $\sim$250 times smaller than the density shift for Cs [24]. For $n \geq 10^{12}$ cm^{-3} (not shown), observed frequency shifts deviate significantly from the linear dependence displayed for $n < 5 \times 10^{11}$ cm^{-3}. Resolving this deviation requires further investigation.

The density-related frequency shift and linewidth-broadening coefficients described above both exceed predicted values based on general S-matrix calculations of s-wave collisions [26, 30]. According to Ref. [26], the clock shift (in Hz) is $\Delta\nu = 4n(\hbar/m)L_s$, where m is the atomic mass, $2\pi\hbar$ is Planck's constant, and L_s is a length that for finite collision temperatures is bound to the order of $1/k$. Here $\hbar k = \sqrt{mE}$ is the thermal collision momentum and E is the collision energy. The bound for the magnitude of the S-matrix is unity. The maximum fractional frequency shift is thus predicted to be -0.5×10^{-24} cm^3, $\sim 1/6^{th}$ of the measured shift. In the low temperature limit and in the absence of resonant scattering, L_s is directly related to the scattering lengths of the two atomic states associated with the clock transition.

Elastic collisions do not account for the relatively large linewidth (w_L) broadening observed here. For inelastic contributions, quenching of the $^3P_1$ excited state was expected to be dominated by $^3P_1 + {}^3P_1$ rather than $^3P_1 + {}^1S_0$ collisions. The quenching rate constant for $^3P_1 + {}^3P_1$ collisions has not been determined previously. An estimate based on the S-matrix formalism described above, however, limits the linewidth broadening coefficient to $\sim 2 \times 10^{-10}$ Hz cm^3, or 140 times smaller than the measured value. Other mechanisms are then most likely responsible for the observed linewidth broadening. This conclusion is supported by the experimental observation that changing the fractional $^3P_1$ density does not significantly alter w_L, indicating $^3P_1 + {}^3P_1$ quenching collisions are not the primary broadening mechanism. We have also experimentally ruled out any significant linewidth contributions due to depolarization of $^3P_1$ to the lower Zeeman level by $^1S_0$ collisions in the presence of the bias magnetic field. Note, however, that the relatively large Sr C_3 coefficient leads to non-negligible p-wave contributions to the $^3P_1 + {}^1S_0$ process even at a temperature $\sim$400 nK. Thus higher order partial waves may make significant contributions to the scattering process. Another experimental observation reveals that for a given range of n, a longer free-flight time (compensated by using a larger initial number of atoms) gives rise to a larger broadening coefficient. Here it is likely that the effec-

TABLE I: Systematic corrections and their associated uncertainties for the absolute frequency of the $^1S_0$ - $^3P_1$ clock transition.

Contributor	Correction (Hz)	Uncertainty (Hz)
mutual beam tilt	0	5
position offset	0	2
velocity	0	4
2nd order Doppler	0	2×10^{-4}
1st order Zeeman	0	0.02
2nd order Zeeman	4	0.3
light shift	0	0.01
blackbody shift	1	0.1
recoil shift	-4775	$< 1\times10^{-3}$
stimulated emission dip	-4	20
probe power balance (I)	-5	15
probe power balance (II)	0	20
density shift	0	2.9
maser calibration	0	1.7
Systematic totals	-4779	33

tive thermal collision momentum k among neighboring atoms is reduced due to their directional correlations in the free-flight expansion, resulting in a larger bound for L_s since the bound is set by $1/k$. We note that the linear fit in Fig. 2 includes the entire data set taken at various free-flight times (5 ms the shortest time).

Figure 4 shows a record of the absolute $^1S_0 - ^3P_1$ optical frequency accumulated over two months. Each entry represents the weighted average of multiple independent measurements. A majority of the measurements are performed in the low density regime ($n < 10^{10}$ cm^{-3}) and all measurements are corrected for the density shift shown in Fig. 3. The final weighted mean is 434 829 121 317 113 Hz, with a statistical uncertainty of 20 Hz. A detailed list of the systematic frequency shifts and their uncertainties are given in Table I. The first four items detail the residual Doppler effect from the atomic motion in free space. The next four items describe frequency shifts due to residual electric and magnetic fields. All have negligible contributions to the present uncertainty. The photon recoil correction is known to 1 mHz. To ensure that corrections for multiple photon recoils are unnecessary, we have verified that no significant shift to the line center occurs for a factor of two decrease in the overall optical power. Lineshape-asymmetry-related frequency shift caused by the stimulated-emission photon recoil is $\sim$4(20) Hz. The other dominant systematic uncertainty arises from the probe beam intensity imbalance. Along with the 20 Hz uncertainty described previously (Table 1, probe power balance II), intensity mismatch leads to preferential multiple scattering in favor of the stronger beam, resulting in a blue shift due to photon recoil of 5(15) Hz (probe power balance I). The overall correction to the measured frequency is therefore -4779 Hz, with a conservatively estimated systematic uncertainty of ~ 33 Hz. Applying this correction, the $^1S_0 - ^3P_1$ transition frequency is $(434\,829\,121\,312\,334 \pm 20_{stat} \pm 33_{sys})$ Hz.

In summary, we have presented the most accurate frequency measurement of a Sr-based optical frequency standard with a detailed investigation of possible systematic sources of error. Using the dense, ultracold sample, we have also performed the first definitive measurement of density-related frequency shifts and linewidth broadening for an optical clock transition.

We thank R. J. Jones and T. Parker for help with absolute frequency measurements and P. Julienne, R. Ciuryło, C. Oates, and A. Gallagher for useful discussions. Funding is provided by ONR, NSF, NASA, and NIST.

[1] L. Hollberg *et al.*, IEEE J. Quant. Electron. **37**, 1502 (2001).
[2] G.Wilpers *et al.*, Phys. Rev. Lett. **89**, 230801 (2002).
[3] H. Katori *et al.*, Phys. Rev. Lett. **91**, 173005 (2003).
[4] H. Katori *et al.*, Phys. Rev. Lett. **82**, 1116 (1999).
[5] T. Binnewies, *et al.*, Phys. Rev. Lett. **87**, 123002 (2001).
[6] T. Mukaiyama *et al.*, Phys. Rev. Lett. **90**, 113002 (2003).
[7] T. H. Loftus *et al.*, Phys. Rev. Lett. **93**, 073003 (2004).
[8] R. J. Rafac *et al.*, Phys. Rev. Lett. **85**, 2462 (2000).
[9] S. A. Diddams *et al.*, Science **293**, 825 (2001).
[10] J. Ye, L.S. Ma, and J. L. Hall, Phys. Rev. Lett. **87**, 270801 (2001).
[11] S. T. Cundiff and J. Ye, Rev. Mod. Phys. **75**, 325 (2003).
[12] F. Ruschewitz *et al.*, Phys. Rev. Lett. **80**, 3173 (1998).
[13] T. Ido and H. Katori,Phys. Rev. Lett. **91**, 053001 (2003). M. Takamoto and H. Katori, Phys. Rev. Lett. **91**, 223001 (2003).
[14] X. Y. Xu *et al.*, J. Opt. Soc. Am. B-Opt. Phys. **20**, 968 (2003).
[15] C. Y. Park and T. H. Yoon, Phys. Rev. A **68**, 055401 (2003).
[16] S. G. Porsev, A. Derevianko, and E. N. Fortson, Phys. Rev. A **69**, 021403 (2004).
[17] T. Trebst *et al.*, IEEE Trans. Instrum. Meas. **50**, 535 (2001).
[18] C. W. Oates, G. Wilpers, and L. Hollberg, LANL arXiv, physics/0401011 (2004).
[19] I. Courtillot *et al.*, Phys. Rev. A **68**, 030501 (2003).
[20] X. Y. Xu *et al.*, Phys. Rev. Lett. **90**, 193002 (2003).
[21] T. Hong *et al.*, LANL arXiv, physics/0409051 (2004). R. Santra *et al.*, LANL arXiv, physics/0411197 (2004).
[22] G. Ferrari *et al.*, Phys. Rev. Lett. **91**, 243002 (2003). I. Courtillot *et al.*, LANL arXiv/0410108 (2004).
[23] C. Fertig and K. Gibble, Phys. Rev. Lett. **85**, 1622 (2000).
[24] Y. Sortais, S. Bize, C. Nicolas, *et al.*, IEEE Trans. Ultrason. Ferroelectr. Freq. Control **47**, 1093 (2000).
[25] P. J. Leo *et al.*, Phys. Rev. Lett. **86**, 3743 (2001).
[26] P. S. Julienne and R. Ciuryło, (private communications, 2004).

[27] G.Wilpers *et al.*, Appl. Phys. B **76**, 149 (2003). U. Sterr *et al.*, LANL arXiv, physics/0411094 (2004).
[28] T. H. Loftus *et al.*, Phys. Rev. A **70**, 063413 (2004).
[29] J. Werner, *et al.* J. Phys. B **26**, 3063 (1993).
[30] P. J. Leo, C. J. Williams, and P. S. Julienne, Phys. Rev. Lett. **85**, 2721 (2000).
[31] J. Ye *et al.*, J. Opt. Soc. Am. B-Opt. Phys. **20**, 1459 (2003).